Critical thickness for the two-dimensional electron gas in $LaTiO_3/SrTiO_3$ superlattices

Jeong Ho You[1,*] and Jun Hee Lee[2]

[1]*Department of Mechanical Engineering, Southern Methodist University, Dallas, Texas, USA*

[2]*Department of Chemistry, Princeton University, Princeton, New Jersey, USA*

(Received 30 May 2013; revised manuscript received 16 September 2013; published 8 October 2013)

Transport dimensionality of Ti d electrons in $(LaTiO_3)_1/(SrTiO_3)_N$ superlattices has been investigated using density functional theory with local spin-density approximation + U method. Different spatial distribution patterns have been found between Ti t_{2g} orbital electrons. The d_{xy} orbital electrons are highly localized near interfaces due to the potentials by positively charged LaO layers, while the degenerate d_{yz} and d_{xz} orbital electrons are more distributed inside $SrTiO_3$ insulators. For $N \geqslant 3$ unit cells (u.c.), the Ti d_{xy} densities of state exhibit the staircaselike increments, which appear at the same energy levels as the d_{xy} flat bands along the Γ-Z direction in band structures. The k_z-independent discrete energy levels indicate that the electrons in d_{xy} flat bands are two-dimensional electron gases (2DEGs) which can transport along interfaces, but they cannot transport perpendicularly to interfaces due to the confinements in the potential wells by LaO layers. Unlike the d_{xy} orbital electrons, the d_{yz} and d_{xz} orbital electrons have three-dimensional (3D) transport characteristics, regardless of $SrTiO_3$ thicknesses. The 2DEG formation by d_{xy} orbital electrons, when $N \geqslant 3$ u.c., indicates the existence of critical $SrTiO_3$ thickness where the electron transport dimensionality starts to change from 3D to 2D in $(LaTiO_3)_1/(SrTiO_3)_N$ superlattices.

DOI: 10.1103/PhysRevB.88.155111 PACS number(s): 73.20.−r, 73.21.−b

I. INTRODUCTION

Recent discoveries of thin metallic layers in heterostructures composed of perovskite oxide insulators have motivated many research activities to understand the origin and properties of conducting carriers.[1–4] In these heterostructures, electrons are strongly localized near interfaces to form two-dimensional electron gases (2DEGs).[5,6] Since 2DEGs have been successfully utilized in semiconductor transport and optical devices,[7,8] perovskite oxide heterostructures with 2DEGs are of great interest to advance oxide electronics with novel functionalities.[4] Especially, $SrTiO_3$-based structures [e.g., $LaAlO_3/SrTiO_3$ (LAO/STO) (Refs. 6 and 9), $LaTiO_3/SrTiO_3$ (LTO/STO) (Refs. 10 and 11), $SrTiNbO_3/SrTiO_3$ (STNO/STO) (Refs. 12–15), etc.] have been intensively investigated and exhibited many intriguing physical properties including high mobility,[5,16,17] superconductivity,[15,18,19] electric-field controlled resistance,[20] novel magnetism,[21–23] and large thermoelectric power.[12–14,24]

In LAO/STO heterostructures, where both constituents are wide band gap insulators, there exists the critical LAO film thickness of 4 unit cells (u.c.) to become conducting.[25] However, LTO/STO heterostructures exhibit a metallic behavior even with a single u.c. of LTO (Refs. 5 and 17). An LTO is a Mott insulator with an occupied Ti $3d^1$ state, while a STO is a band gap insulator with an empty Ti $3d^0$ state. When a LTO is adjoined to a STO, Ti cations in TiO_2 layers between adjacent LaO and SrO layers begin to have an averaged valence of $3d^{0.5}$ (Refs. 26 and 27). This electronic reconstruction induces the metallic LTO/STO interfaces with the carrier density of $\sim 0.5e$/u.c. per interface.[5] Ohtomo *et al.*[1] have found the leakage of Ti $3d$ electrons from the interfacial TiO_2 layers into a few unit cells of STO. Density functional theory (DFT) calculations have revealed that the extent of Ti $3d$ electrons strongly depends on the screening of potentials induced by positively charged LaO layers.[28–30] Tunability of transport properties has been investigated by fractional doping such as $La_xSr_{1-x}TiO_3/SrTiO_3$ and $SrTi_yNb_{1-y}O_3/SrTiO_3$ structures.[11–13,31]

In this study, we investigate the effects of STO spacers on transport dimensionality in $(LTO)_1/(STO)_N$ superlattices grown on STO substrate. Since both LTO and STO have a common TiO_2 layer, the $(LTO)_1/(STO)_N$ superlattices have a LaO layer replacing a SrO layer in every $(N + 1)$ u.c. along the [001] growth direction. With varying the STO spacer thickness, we are controlling the separation distance between the LaO-induced potential wells to examine the changes of electron transport properties.

II. CALCULATION DETAILS

DFT calculations have been used to investigate the $(LTO)_1/(STO)_N$ superlattices with various STO thicknesses as N = 1–10 u.c. All calculations were performed using the Vienna *Ab initio* Simulation Package (VASP)[32,33] with the projector-augmented wave approach,[34] the energy cutoff of 500 eV, and the rotationally invariant local spin-density approximation (LSDA) + U method.[35] We used U = 5 eV and J = 0.64 eV for Ti d states,[30,36] and U_f = 11 eV and J_f = 0.68 eV for La f states.[30] The in-plane (xy plane) lattice constants were fixed as the experimental value of 3.91 Å for cubic STO to simulate the boundary condition by the STO substrate.[1] The out-of-plane (z direction) lattice vector was optimized within the tetragonal $P4mm$ space group, and all ionic positions were relaxed until all Hellmann-Feynman forces were smaller than 5 meV/Å. After self-consistent calculations were performed with a $6 \times 6 \times n$ k-point grid where $n \approx 6/(N + 1)$ to optimize the lattice vector and ionic positions, non self-consistent calculations were carried out with a finer k-point grid of $24 \times 24 \times n$ where $n \approx 24/(N + 1)$.

III. RESULTS AND DISCUSSION

The calculated relaxed structure for the $(LTO)_1/(STO)_8$ superlattice is shown in Fig. 1(a) as an example. In the relaxed structure, the negatively charged O atoms move toward the

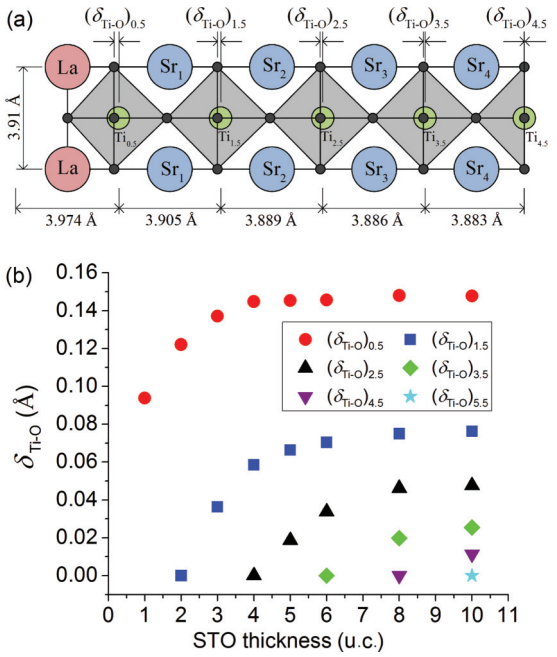

FIG. 1. (Color online) (a) Calculated relaxed structure for the $(LTO)_1/(STO)_8$ superlattice as an example. (b) Relative Ti-O displacements (δ_{Ti-O}) as a function of STO thickness in $(LTO)_1/(STO)_N$ superlattices.

positively charged LaO layer due to Coulomb force. This ferroelectriclike TiO_6 octahedra distortion is known to provide ionic screening in addition to electronic screening to the potentials by LaO layers, and, as a result, the Ti d electrons are spread widely over a few unit cells of STO.[28–30] The relative Ti-O displacements (δ_{Ti-O}) are shown in Fig. 1(b) as a function of STO thickness. The largest δ_{Ti-O} always occurs at the interfacial TiO_2 layer ($Ti_{0.5}$), and the magnitude of δ_{Ti-O} decays rapidly as moving away from the interface. As the STO thickness increases, the magnitude of δ_{Ti-O} increases and gets converged. For $N = 3$–4 u.c., the magnitude of $(\delta_{Ti-O})_{0.5}$ is converged to ~0.14 Å.

Spatial distributions of Ti d electrons have been calculated for different STO spacer thicknesses, as shown in Fig. 2. The d electron charges are obtained by integrating the occupied states in Ti $3d$ densities of states (DOS; shown in Fig. 3) and normalized to have $0.5e$/u.c. per interface [i.e., $1e$/u.c. per LTO cell in $(LTO)_1/(STO)_N$ superlattices]. The positively charged LaO layers are located at the periodic positions of $0, \pm(N+1), \pm2(N+1), \ldots$. Different distribution patterns can be observed between Ti t_{2g} orbitals. The d_{xy} orbital electrons are highly localized near the interfaces, and its occupancy decays fast inside the STO insulators. With increasing the STO spacer thickness, the neighboring d_{xy} electrons become almost separated. As an example, in the $(LTO)_1/(STO)_{10}$ superlattice, the d_{xy} electron charges are only $0.0055e$ and $0.0051e$ at the $Ti_{4.5}$ and $Ti_{5.5}$ sites, respectively. The high occupancy at the interfaces indicates that the d_{xy} orbital is strongly influenced by the LaO-induced potential wells. In contrast to the d_{xy} orbital, the degenerate d_{yz} and d_{xz} orbitals are more occupied inside the STO insulators. Also, the occupancy of d_{yz} (d_{xz}) orbital decreases drastically and becomes almost homogeneous with the increase of STO thickness.

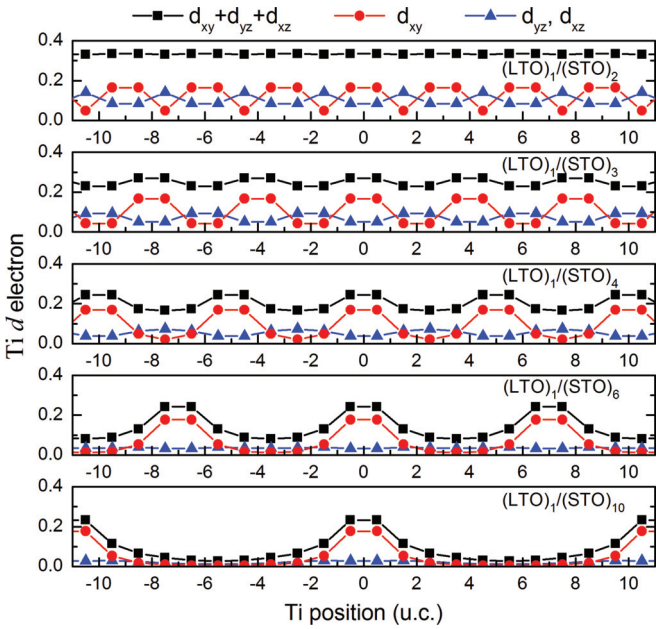

FIG. 2. (Color online) Spatial distributions of Ti $3d$ electrons in $(LTO)_1/(STO)_N$ superlattices. Ti d electron densities are normalized to have $0.5e$/u.c. per interface. The positively charged LaO layers are located at the periodic positions of $0, \pm(N+1), \pm2(N+1), \ldots$.

Figure 3 shows the calculated Ti $3d$ DOS for conduction bands with various STO spacer thicknesses. The Fermi level is at 0 eV. At each Ti site, the DOS with spin-up (spin-down) states is shown in the upper (lower) panel. From the integration of DOS between midgap and the Fermi level, the d electron density of $\sim 0.7e$/u.c. has been obtained. In the $(LTO)_1/(STO)_1$ superlattice, the DOS for both d_{xy} and d_{yz} (d_{xz}) orbitals gradually increases with energy as shown in Fig. 3(a). In the

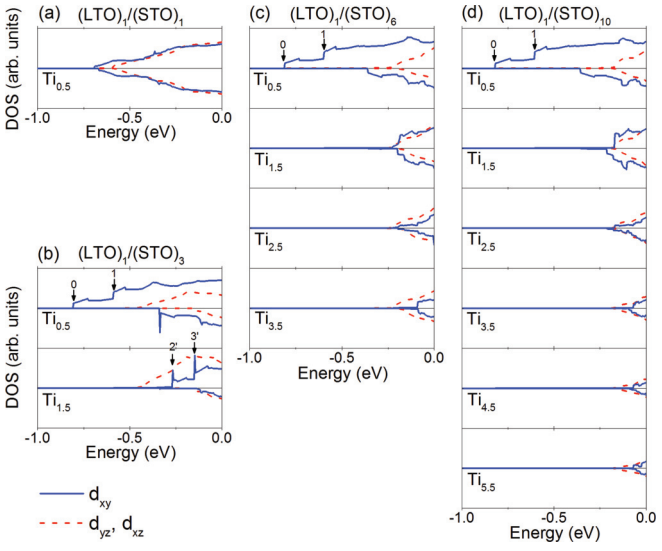

FIG. 3. (Color online) Ti $3d$ DOS for conduction bands at Ti atoms for (a) $(LTO)_1/(STO)_1$, (b) $(LTO)_1/(STO)_3$, (c) $(LTO)_1/(STO)_6$, and (d) $(LTO)_1/(STO)_{10}$ superlattices. The Fermi level is at 0 eV. At each Ti site, the DOS with spin-up (spin-down) states is shown in the upper (lower) panel. The d_{xy} orbital is blue (solid line), while the degenerate d_{yz} and d_{xz} states are red (dashed line).

$(LTO)_1/(STO)_3$ superlattice, the shape of d_{xy} DOS becomes different from the d_{yz} (d_{xz}) DOS. As shown in Fig. 3(b), the DOS of d_{xy} spin-up states at the $Ti_{0.5}$ site exhibits the staircaselike increments at −0.82 eV and −0.60 eV (marked as 0 and 1). Interestingly, these staircaselike increments remain the same for thicker STO spacers, as shown in Figs. 3(c) and 3(d). Such a staircase increment in DOS is a well-known feature of 2DEGs with quantized energy levels due to wave function confinements. In the $(LTO)_1/(STO)_N$ superlattices with $N \geqslant 3$ u.c., the d_{xy} orbital electrons at $Ti_{0.5}$ sites are 2DEGs confined in the LaO-induced potential wells with the discrete energy levels of −0.82 eV and −0.60 eV.

In the $(LTO)_1/(STO)_3$ structure, the d_{xy} DOS has other staircase increments at the $Ti_{1.5}$ site but at higher energy levels of −0.287 eV and −0.162 eV [marked as $2'$ and $3'$ in Fig. 3(b)]. This can be explained by the distributions of 2DEGs in a wedge/triangular potential well; electrons at low energy are localized near the potential valley, but electrons at high energy stay away from the potential valley.[10,37] The presence of d_{xy} 2DEGs at discrete energy levels also explains the multichannel conduction from experiments.[5] The DOS of d_{yz} (d_{xz}) orbital does not show staircaselike increments. Generally, it increases with energy indicating that the d_{yz} (d_{xz}) orbital has 3D transport characteristics.

To confirm the transport dimensionality of d orbitals, the transport directivity has been investigated by calculating electron effective masses from band structures. Figure 4 shows the calculated band structures for spin-up states within the first Brillouin zone. The Fermi level is at 0 eV. In the $(LTO)_1/(STO)_1$ structure, the d_{xy} band is the lowest conduction band at −0.714 eV at the Γ point, and the d_{yz} (d_{xz}) band is the second lowest conduction band at −0.605 eV. Using the parabolic approximation near the Γ point, the electron effective masses

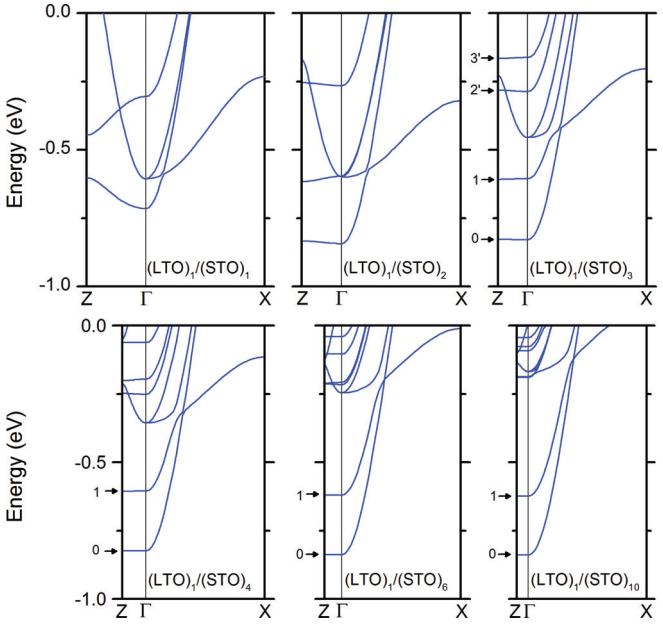

FIG. 4. (Color online) Band structures of $(LTO)_1/(STO)_N$ superlattices for spin-up states within the first Brillouin zone. Only conduction bands are shown here. The Fermi level is at 0 eV. The bands 0, 1, $2'$, and $3'$ correspond to the increments in d_{xy} DOS in Fig. 3.

of the lowest d_{xy} band are calculated as $m_{xx} = 0.40\ m_0$ and $m_{zz} = 2.67\ m_0$, parallel and perpendicular to the interfaces, respectively. In the $(LTO)_1/(STO)_2$ structure, the lowest d_{xy} band moves down to −0.83 eV, which is lower than the d_{yz} (d_{xz}) band by 0.246 eV at the Γ point. In the $(LTO)_1/(STO)_2$ structure, the electron effective mass of the lowest d_{xy} band has increased to $m_{zz} = 10.8\ m_0$ perpendicular to the interfaces, but it remains the same as $m_{xx} = 0.40\ m_0$ along the interfaces. In the $(LTO)_1/(STO)_3$ structure, the lowest d_{xy} band (marked as 0) becomes almost flat along the Γ-Z direction, which implies that the kinetic energy is independent from k_z. Since the effective mass is inversely proportional to the band curvature at the Γ point, the electrons in the lowest d_{xy} band in the $(LTO)_1/(STO)_3$ structure are extremely heavy to transport perpendicularly to the interfaces, but they can still transport along the interfaces with the effective mass of $m_{xx} = 0.40\ m_0$. Furthermore, the lowest d_{xy} band in the $(LTO)_1/(STO)_3$ band structure is at −0.83 eV, which is very close to the first staircase increment in the d_{xy} spin-up DOS at the $Ti_{0.5}$ site [see Fig. 3(b)]. Therefore, the lowest d_{xy} band in the $(LTO)_1/(STO)_3$ superlattice is the 2DEG, which can travel only along the interface due to the confinement by the LaO-induced potential well.

The second lowest d_{xy} band is also the 2DEG at −0.61 eV (marked as 1), corresponding to the second staircase increment in the d_{xy} DOS at the $Ti_{0.5}$ site [see Fig. 3(b)]. These two lowest d_{xy} bands (0 and 1) also remain the same for $N \geqslant 3$ u.c., as shown in Fig. 4. Unlike d_{xy} bands, the d_{yz} (d_{xz}) bands have constant electron effective masses as $m_{xx} = 0.50\ m_0$ and $m_{zz} = 0.45\ m_0$ for all STO thicknesses, which confirms that the d_{yz} (d_{xz}) orbital electrons have 3D transport property in $(LTO)_1/(STO)_N$ superlattices.

Electron densities of d orbitals are shown in Fig. 5 as a function of STO thickness. In the $(LTO)_1/(STO)_1$ superlattice, the d_{xy} electron density is slightly higher than the d_{yz} (d_{xz}) electrons. As the STO thickness increases, the d_{xy} electron density increases, while the d_{yz} (d_{xz}) electron density decreases. Since the 2DEG is formed by d_{xy} orbital electrons when $N \geqslant 3$ u.c. only and the d_{yz} (d_{xz}) orbital electrons always

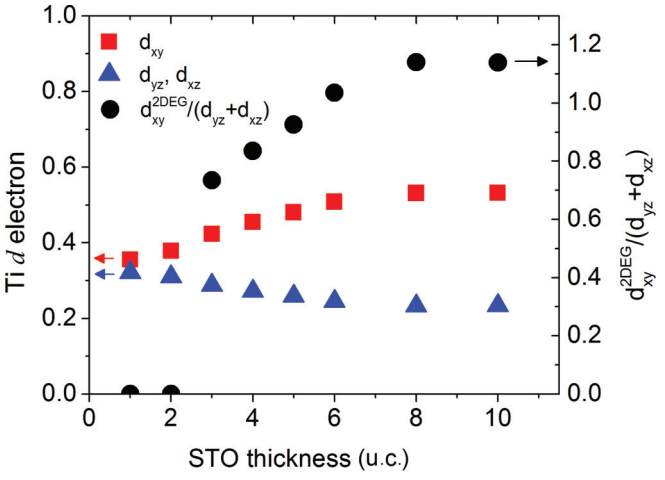

FIG. 5. (Color online) Normalized electron densities of d_{xy} and d_{yz} (d_{xz}) orbitals as a function of STO thickness and the ratio of 2DEG to 3D electrons as $d_{xy}^{2DEG}/(d_{yz} + d_{xz})$ with $d_{xy}^{2DEG} = 0$ for $N < 3$ u.c.

have 3D transport characteristic, the transport dimensionality of $(LTO)_1/(STO)_N$ superlattices starts to change from 3D to 2D at $N = 3$ u.c. The ratio of 2D to 3D electrons can be estimated as $d_{xy}^{2DEG}/(d_{yz} + d_{xz})$ with taking $d_{xy}^{2DEG} = 0$ for $N < 3$ u.c., as shown in Fig. 5. The convergence of d_{xy} and $(d_{yz} + d_{xz})$ electron densities at $N = 8$ u.c. is due to the large separation distance between the neighboring potentials.

IV. CONCLUSION

The effects of STO spacer thickness on the transport dimensionality of d orbital electrons in $(LTO)_1/(STO)_N$ superlattices have been investigated using DFT calculations with the LSDA + U method. The d_{xy} orbital electrons are highly localized near interfaces due to the potentials by the positively charged LaO layers, while the degenerate d_{yz} and d_{xz} orbital electrons are more distributed inside the STO insulators. As the STO thickness increases, the occupancy of d_{yz} (d_{xz}) orbital decreases drastically and becomes almost uniform. For $N \geqslant 3$ u.c., the Ti d_{xy} DOS shows the staircaselike increments, which appear at the same energy levels of d_{xy} flat bands along Γ-Z direction in band structures. These k_z-independent discrete energy levels indicate that the electrons in d_{xy} flat bands are 2DEGs that can transport along interfaces but cannot transport perpendicularly to interfaces due to the confinements in the potential wells by LaO layers. Unlike d_{xy} orbital electrons, the d_{yz} and d_{xz} orbital electrons always have 3D transport characteristics. The formation of the d_{xy} 2DEG for $N \geqslant 3$ u.c. indicates that the electron transport dimensionality in $(LaTiO_3)_1/(SrTiO_3)_N$ superlattices starts to change from 3D to 2D with the STO thickness of 3 u.c.

*Corresponding author: jyou@smu.edu

[1] A. Ohtomo, D. A. Muller, J. L. Grazul, and H. Y. Hwang, Nature **419**, 378 (2002).
[2] A. Ohtomo and H. Y. Hwang, Nature **427**, 423 (2004).
[3] N. Nakagawa, H. Y. Hwang, and D. A. Muller, Nat. Mater. **5**, 204 (2006).
[4] J. Mannhart and D. G. Schlom, Science **327**, 1607 (2010).
[5] J. S. Kim, S. S. A. Seo, M. F. Chisholm, R. K. Kremer, H. U. Habermeier, B. Keimer, and H. N. Lee, Phys. Rev. B **82**, 201407(R) (2010).
[6] A. D. Caviglia, S. Gariglio, C. Cancellieri, B. Sacepe, A. Fete, N. Reyren, M. Gabay, A. F. Morpurgo, and J. M. Triscone, Phys. Rev. Lett. **105**, 236802 (2010).
[7] S. L. Chuang, *Physics of Optoelectronic Devices* (John Wiley & Sons, Inc., New York, 1995).
[8] J. H. Davies, *The Physics of Low-dimensional Semiconductors: An Introduction* (Cambridge University Press, New York, 1997).
[9] S. Su, J. H. You, and C. Lee, J. Appl. Phys. **113**, 093709 (2013).
[10] J. Biscaras, N. Bergeal, S. Hurand, C. Grossetete, A. Rastogi, R. C. Budhani, D. LeBoeuf, C. Proust, and J. Lesueur, Phys. Rev. Lett. **108**, 247004 (2012).
[11] W. S. Choi, S. Lee, V. R. Cooper, and H. N. Lee, Nano Lett. **12**, 4590 (2012).
[12] H. Ohta, S. Kim, Y. Mune, T. Mizoguchi, K. Nomura, S. Ohta, T. Nomura, Y. Nakanishi, Y. Ikuhara, M. Hirano, H. Hosono, and K. Koumoto, Nat. Mater. **6**, 129 (2007).
[13] Y. Mune, H. Ohta, K. Koumoto, T. Mizoguchi, and Y. Ikuhara, Appl. Phys. Lett. **91**, 192105 (2007).
[14] H. Ohta, Y. Mune, K. Koumoto, T. Mizoguchi, and Y. Ikuhara, Thin Solid Films **516**, 5916 (2008).
[15] Y. Kozuka, M. Kim, C. Bell, B. G. Kim, Y. Hikita, and H. Y. Hwang, Nature **462**, 487 (2009).
[16] M. Basletic, J. L. Maurice, C. Carretero, G. Herranz, O. Copie, M. Bibes, E. Jacquet, K. Bouzehouane, S. Fusil, and A. Barthelemy, Nat. Mater. **7**, 621 (2008).
[17] R. Ohtsuka, M. Matvejeff, K. Nishio, R. Takahashi, and M. Lippmaa, Appl. Phys. Lett. **96**, 192111 (2010).
[18] N. Reyren, S. Thiel, A. D. Caviglia, L. F. Kourkoutis, G. Hammerl, C. Richter, C. W. Schneider, T. Kopp, A. S. Ruetschi, D. Jaccard, M. Gabay, D. A. Muller, J. M. Triscone, and J. Mannhart, Science **317**, 1196 (2007).
[19] J. Biscaras, N. Bergeal, A. Kushwaha, T. Wolf, A. Rastogi, R. C. Budhani, and J. Lesueur, Nature Commun. **1**, 89 (2010).
[20] A. D. Caviglia, S. Gariglio, N. Reyren, D. Jaccard, T. Schneider, M. Gabay, S. Thiel, G. Hammerl, J. Mannhart, and J. M. Triscone, Nature **456**, 624 (2008).
[21] A. Brinkman, M. Huijben, M. Van Zalk, J. Huijben, U. Zeitler, J. C. Maan, W. G. Van der Wiel, G. Rijnders, D. H. A. Blank, and H. Hilgenkamp, Nat. Mater. **6**, 493 (2007).
[22] L. Li, C. Richter, J. Mannhart, and R. C. Ashoori, Nat. Phys. **7**, 762 (2011).
[23] J. A. Bert, B. Kalisky, C. Bell, M. Kim, Y. Hikita, H. Y. Hwang, and K. A. Moler, Nat. Phys. **7**, 767 (2011).
[24] B. Jalan and S. Stemmer, Appl. Phys. Lett. **97**, 042106 (2010).
[25] S. Thiel, G. Hammerl, A. Schmehl, C. W. Schneider, and J. Mannhart, Science **313**, 1942 (2006).
[26] H. Ishida and A. Liebsch, Phys. Rev. B. **77**, 115350 (2008).
[27] V. R. Cooper, Phys. Rev. B **85**, 235109 (2012).
[28] P. Larson, Z. S. Popović, and S. Satpathy, Phys. Rev. B **77**, 245122 (2008).
[29] D. R. Hamann, D. A. Muller, and H. Y. Hwang, Phys. Rev. B **73**, 195403 (2006).
[30] S. Okamoto, A. J. Millis, and N. A. Spaldin, Phys. Rev. Lett. **97**, 056802 (2006).
[31] P. V. Ong, J. Lee, and W. E. Pickett, Phys. Rev. B **83**, 193106 (2011).
[32] G. Kresse and J. Furthmüller, Phys. Rev. B **54**, 11169 (1996).
[33] G. Kresse and D. Joubert, Phys. Rev. B **59**, 1758 (1999).
[34] P. E. Blöchl, Phys. Rev. B **50**, 17953 (1994).
[35] A. I. Liechtenstein, V. I. Anisimov, and J. Zaanen, Phys. Rev. B **52**, R5467 (1995).
[36] T. Mizokawa and A. Fujimori, Phys. Rev. B **51**, 12880 (1995).
[37] Z. S. Popovic and S. Satpathy, Phys. Rev. Lett. **94**, 176805 (2005).